

Modal Dispersion Curves in the Ocean

D. Cassereau^a, P. Roux^b, and F.-D. Philippe^a

^a *Laboratoire Ondes et Acoustique, Université Paris 7 - CNRS UMR 7587 - ESPCI, Paris, FRANCE*

^b *Marine Physical Laboratory - Scripps Institution of Oceanography, La Jolla, U.S.A.*
didier.cassereau@espci.fr

Introduction

In underwater acoustics, the pressure field P_ω at a frequency $f = 2\pi\omega$ is decomposed under the propagating modes as follows:

$$P_\omega(R) = \sum_{m=1}^M a_m \exp(ik_m R), \quad (1)$$

where M is the number of modes, R is the source-receiver range, and k_m is the wavenumber associated to mode m . For simplicity, we neglect the attenuation in the waveguide.

Like in many high-resolution techniques, the data are issued from a towed source providing a horizontal synthetic aperture; for the n^{th} position of the source given by $R=R_0+nd$, we measure the corresponding pressure $P_\omega[n]$ received on the receiver.

Replacing R in (1) by its expression, we obtain an equivalent formulation of (1) as

$$P_\omega[n] = \sum_{m=1}^M \tilde{a}_m z_m^n, \text{ with } z_m = \exp(ik_m d). \quad (2)$$

In this equation, we have M unknown amplitudes \tilde{a}_m and M unknown phases z_m . Consequently, we need at least $2M$ data points in order to solve this system. Using $2M$ data points, the problem can be seen as the inversion of a $2M$ -equation system. This system is linear with respect to \tilde{a}_m , but it is highly nonlinear with respect to z_m . This nonlinearity makes the inversion difficult and highly sensitive to noise.

The method we propose is similar to the Prony method and is based on the following steps:

- we start from the first M equations of (2), and write the \tilde{a}_m as a function of the data $P_\omega[n]$ and phases z_m ,
- we continue with the last M equations of (2), in which the \tilde{a}_m are replaced by their expression.

These two steps are symbolic manipulations of (2); there is no numerical treatment here. Of course, we obtain a system of M equations with M unknown phases z_m , that is highly nonlinear. Anyway, we can show that this system is linear with respect to the Elementary Symmetric Polynomials defined by:

$$E_1 = \sum_{i=1}^M z_i, E_2 = \sum_{i=1}^M \sum_{j=i+1}^M z_i z_j, \dots, E_M = \prod_{i=1}^M z_i. \quad (4)$$

The next steps of our inversion algorithm are:

- numerical inversion of this linear system and computation of the E_m ,
- calculation of the phases z_m as the complex roots of a polynomial of degree M , whose coefficients are the E_m .

The determination of the E_m results from the inversion of a linear system; thus there is no particular difficulty here in the numerical implementation. Then the final resolution step reduces to the search of the roots of a polynomial,

which can be performed from multiple and stable numerical algorithms. In fact, the most complex step was the symbolic manipulations that were needed to obtain the last formulation given above.

Representation of the multi-valued solutions

As described in the two previous sections, our inversion method (with or without holographic array processing) yields the numerical determination of the phase variables $z_m = \exp(ik_m d)$. Now, the calculation of the corresponding k_m is not straightforward, even in the case of a well-known distance d . This is due to the fact that the phase of a complex number is known, up to a multiple of 2π . As an immediate consequence, the wavenumbers k_m are given by

$$k_m d = \text{phase}(z_m) + 2p\pi, \quad (5)$$

where p can be any positive or negative integer.

In order to find the exact wavenumbers, we take advantage of the large number of data points. Indeed, our inversion algorithm is performed from $2M$ data points, and we can choose multiple subsets of $2M$ equally points in the total aperture L covered by the moving source. We finally proceed in the following manner:

- we choose d and a subset of $2M$ data points such that we have $(2M-1)d < L$, on which we run our inversion algorithm.
- once the z_m are known, we calculate all possible values of k_m inside a reasonable range, taking into account the multi-valued solutions,
- we restart the last two steps for all possible subsets of points for a given value of d , and also for different values of d if possible.

The basic idea of this procedure is to cumulate the multi-valued wavenumbers obtained from different subsets of data points, and draw a histogram of all possible solutions. For an effective solution, all individual histograms will have a peak at the same k -position, thus resulting in a cumulative high peak on the final result. For a non-pertinent solution resulting from the multi-valuation, it will be spread along the k axis from one particular histogram to another one, and we do not expect to see any peak in this case.

As a matter of fact, a strong peak detection on the final histogram allows to separate the actual solution from virtual solutions that result from multi-valuation.

Numerical results

Data are obtained from a numerical simulation in a 60-m deep Pekeris waveguide using the Kraken normal mode code at a frequency of 200 Hz. The bottom sound speed, density and attenuation are 2000 m/s, 2000 kg/m³ and 0.1 dB/λ. The source is towed away from the receiver on a total aperture $L=1500$ m with an initial distance to the receiver $R_0=3000$ m; the depth of the source is 15 m. The water sound speed and density are 1500 m/s and 1000 kg/m³.

Fig.1 shows a typical cumulative histogram obtained from our inversion technique with a single receiver in the absence of noise. The sharp peaks correspond to the actual modes in the waveguide, in the range $[0.55 \text{ m}^{-1}-0.95 \text{ m}^{-1}]$. The portion of the histogram between 0.85 and 0.95 m^{-1} gives us an estimation of the average noise level resulting from the multi-valuation treatment. We then define a threshold with respect to this average noise level in order to detect the peaks in the histogram.

In Fig. 1, we clearly identify 11 different peaks that rise high above the average noise level. These different peaks correspond to the actual wavenumbers of the waveguide.

In Fig. 2, random white noise is added on the simulated data points (SNR=20 dB). Comparing Figs. 1 and 2, we see that the detection of modes is more difficult in the presence of noise; the average noise level does not change between the different figures, but the height of the peaks decreases as noise increases. Some peaks are no more detected, and the two highest modes can not be distinguished, as in Fig. 1. If we use a detection based on a threshold compared to the average noise level, we can expect that some modes are missed in the case of a highly noisy propagation in the waveguide.

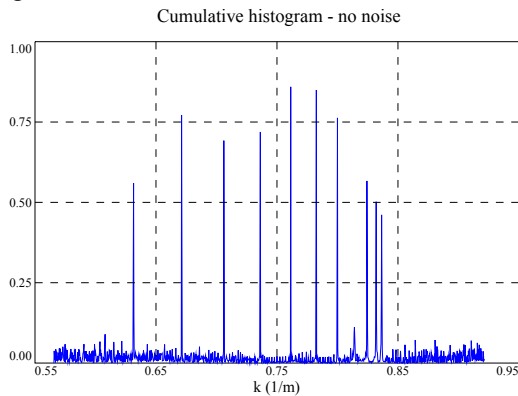


Figure 1: typical cumulative histogram without noise.

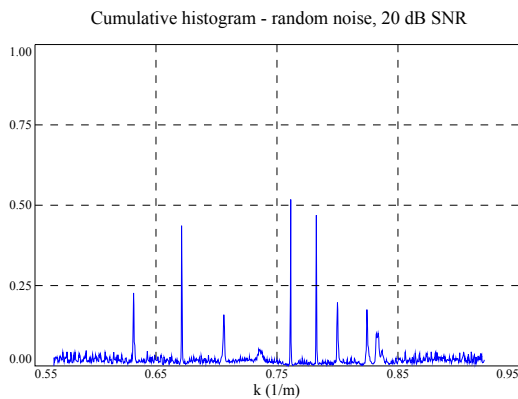


Figure 2: same as figure 1, with a random white noise, 20 dB SNR.

Modal dispersion curves in the ocean

In the previous sections, we considered only monochromatic signals at the frequency of 200 Hz. The simulated data points have been calculated using a single-frequency propagation model.

We investigate now the case of broadband signals received from a horizontal synthetic aperture. To do so, the previous inversion procedure is repeated for all the frequencies that

are effectively present in the temporal signals received on the array. This yields a series of wavenumbers for each frequency that can be represented in the (k, f) space to obtain the modal dispersion curves of the waveguide. These dispersion curves are very important because they contain much information about the physical properties of the waveguide and bottom.

In practice, the simulated data points are now obtained from a transient propagation model based on the Kraken normal mode code. The central frequency is 200 Hz, and the effective bandwidth is in the range $[175-225 \text{ Hz}]$. The computation of the dispersion curves has been limited to this frequency range. The length of the horizontal aperture $L=1500 \text{ m}$ is the same as before.

Figs. 3a and 3b show the modal dispersion curves obtained in the absence of noise and in the case of a 20-dB SNR, respectively. On these two figures, we see the classical structure of the dispersion curves in the waveguide, and the degradation due to the presence of noise.

Conclusion

In this work, we have presented a numerical procedure to calculate the propagating wavenumbers in a waveguide, and the resulting dispersion curves. These results may be useful in underwater acoustics, since dispersion curves contain information about the waveguide properties.

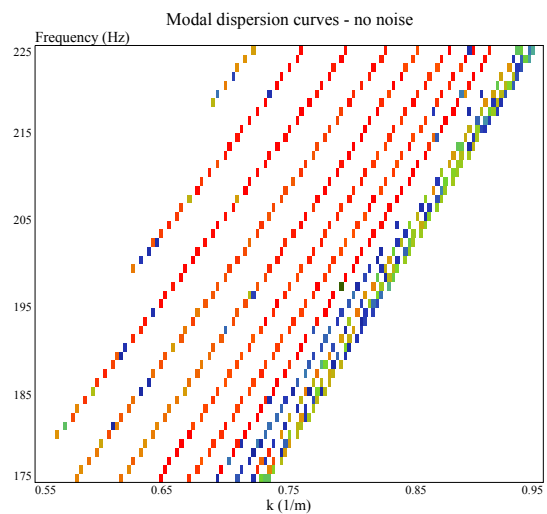


Figure 3a: dispersion curves without noise.

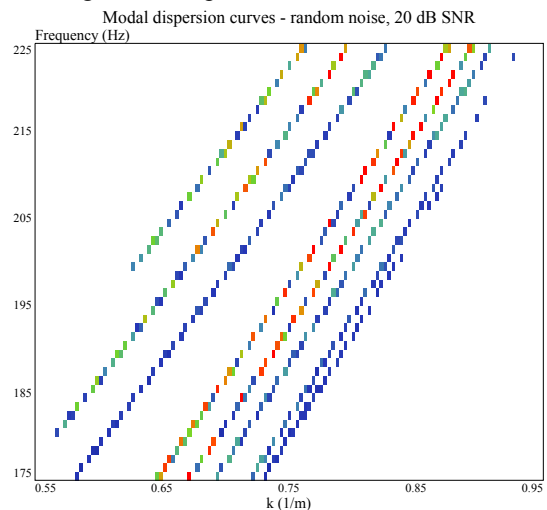


Figure 3b: dispersion curves with a 20-dB SNR.